Electrically Controlled Plasmonic Switches and Modulators

Alexandros Emboras, Claudia Hoessbacher, Christian Haffner, Wolfgang Heni, Ueli Koch, Ping Ma, Yuriy Fedoryshyn, Jens Niegemann, Christian Hafner, and Jurg Leuthold, *Fellow, IEEE*

(Invited Paper)

***Abstract*—Plasmonic modulators and switches have recently attracted considerable attention because they offer ultracompact size, high bandwidths, and potentially low-power consumption. In this paper, we review and compare the current state of the art of plasmonic switches and discuss the various physical phenomena that are used to perform efficient switching. More precisely, we discuss plasmonic devices based on the thermal effect, the free carrier dispersion effect, the Pockels effect, phase change materials and switching caused by electrochemical metallization.**

***Index Terms*—Integrated photonics, plasmonic switches, thermo-plasmonic, free carrier dispersion, Pockels effect, electrochemical metallization, phase change effect.**

I. Introduction

An ideal optical switch should feature a small footprint, offer high speed operation and operate with the least possible power consumption. However, to this day, optical switches have relatively large footprints compared to λ and often require significant power. State-of-the art in telecommunications circuit switches are mostly based on MEMS technology, have footprints of several hundreds of μm^2 and consume several Watts of power to be operated [1]. Other commercial integrated optical switches typically are based on lithium niobate and come with footprints of several cm^2 [2]–[4]. More advanced approaches have shown footprints of several mm^2 [5], [6]. While all of these approaches show a trend towards more compact sizes, the overall dimensions are still too large in view of a cointegration with electronics. Today, some 100 electrical devices fit onto a single μm^2. If optical devices should ever be cointegrated with electronics, then their footprint needs to be dramatically reduced as CMOS costs are calculated per μm^2.

To further reduce the footprint, resonantly operated devices have been suggested. They either take advantage of the slow light effect in photonic crystal waveguides [7], [8] or they are relying on resonant ring filter configurations. The latter have recently demonstrated operation up to 40 Gbit/s on a footprint of as little as $\sim$30 μm^2 [9]–[11]. However, resonant structures usually are very sensitive to temperature changes and therefore require active temperature control.

Fig. 1. Physical effects that have been used to perform plasmonic switching.

More recently, plasmonics has emerged as a potential solution to some of those issues [12]–[24]. In plasmonics, information is carried by surface plasmons polaritons (SPP). SPPs are electromagnetic waves strongly coupled to the free electrons at the metal surface. They are propagating along the metal-dielectric interface and can be manipulated below the diffraction limit. Combining the propagation properties of optical waves with the high localization of electronic waves, plasmons can achieve extremely large field confinement. This confinement property can be exploited to develop novel plasmonic devices with footprints of μm^2 [13], [19], [25]–[27].

This work is an attempt to cover the key phenomena which are currently considered to electrically control plasmonic switches and modulators, Fig. 1. It can be seen that various physical effects may be used to change the refractive index or absorption characteristic of plasmonic waveguides. Below we will discuss the five effects listed in Fig. 1 one by one and give recent implementation examples.

And while we can only give a few examples, it needs to be understood that each effect can be exploited in many possible configurations. For instance, a phase-modulation effect can be exploited in a straight phase modulator device for phase modulation, but it could as well be exploited for switching or amplitude modulation in a Mach-Zehnder interferometer or for intensity

Manuscript received October 4, 2014; revised November 21, 2014; accepted December 6, 2014. This work was supported in part by the U.S. Department of Commerce under Grant BS123456.

The authors are with the Institute of Electromagnetic Fields, ETH Zürich, 8092 Zürich, Switzerland (e-mail: alexandros.emboras@ief.ee.ethz.ch; claudia.hoessbacher@ief.ee.ethz.ch; christian.haffner@ief.ee.ethz.ch; wolfgang.heni@ief.ee.ethz.ch; ueli.koch@ief.ee.ethz.ch; ping.ma@ief.ee.ethz.ch; yuriy.fedoryshyn@ief.ee.ethz.ch; jens.niegemann@ief.ee.ethz.ch; christian.hafner@ief.ee.ethz.ch; juerg.leuthold@ief.ee.ethz.ch).

Color versions of one or more of the figures in this paper are available online at http://ieeexplore.ieee.org.

Digital Object Identifier 10.1109/JSTQE.2014.2382293

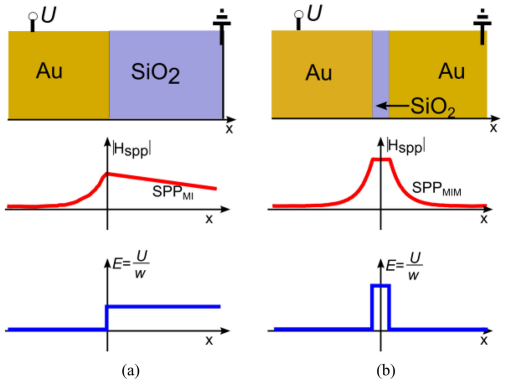

Fig. 2. Typical plasmonic device structures used for optical modulation: (a) metal-insulator structure along with the spatial distribution of the H field intensity profile of the fundamental SPP mode and the static electric field, U/w.; (b) metal-insulator-metal structure along with the spatial distribution of the H field intensity profile of the fundamental SPP mode and the static electric field, U/w.

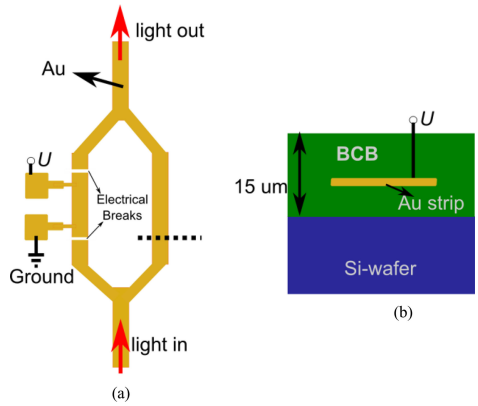

Fig. 3. (a) Top view schematic of the Mach-Zehnder thermoplasmonic switch; (b) cross section of the active device [15].

modulation (on-off switching) in a ring filter. Of course it is impossible to cover all possible implementations and aspects and we therefore ask for an understanding that only few of the many great work in the field can be cited here.

II. Active Plasmonic Structures

Active plasmonic switches require an appropriate plasmonic waveguide technology that allows for optical guiding but also for a control of the active area. There are basically two plasmonic waveguide structures that were found to be useful, see Fig. 2. The first one is rather simple and consists of a metal-insulator (MI) interface. The plasmonic field is strongly confined at the MI interface and exponentially decays with increasing distance from the interface. The losses of MI plasmonic waveguides are mainly determined by the extent to which the field resides in the metal. Typical propagation lengths are in the order of a few tens of μm. Another popular plasmonic waveguide is based on a metal-insulator-metal (MIM) stack. This type of structure offers a strong subwavelength confinement of the plasmon. As an advantage, the two metals can be used as electrodes across which an electrical field can be applied. This way the electric field, *U/w* (modulating voltage *U*, gap width *w*) drops off across the area where the plasmon field is strongest, thus providing an excellent overlap of electric and plasmonic field, see Fig. 2(b). Moreover, metals have a very low resistivity and thus offer a bandwidth that is not limited by RC time constants, which is not easily achievable by doped Si. Therefore, the structure is rather unique for electro-optical devices which are operated below the diffraction limit and at high bandwidths. However, such plasmonic structures must balance high field confinement with optical losses (the propagation length is a few μm). The latter can be addressed by choosing the right materials and a proper design [28]–[36].

III. Thermo-Plasmonic Effect

The thermo-plasmonic effect allows operation of a switch with a very compact characteristic length. This is due to the fact that a heating wire can act as a plasmonic waveguide. The heating wire changes the refractive index of the dielectric cladding around the wire; this is exactly where the largest part of the SPP mode is confined to [37]. As a result one has a large overlap between the electromagnetic field of the plasmonic mode and the thermally induced energy. Taking advantage of this unique property, several devices have been demonstrated but only few of them can be reviewed here [15], [37]–[43]. It is worth noting that typical devices based on the thermo-plasmonic effect show high extinction ratios but only moderate switching times (in the μs range) and relatively high power consumption (few mW).

In 2004, Nikolajsen *et al*. [15] demonstrated the first thermo-plasmonic switch relying on a Mach-Zehnder interferometer as sketched in Fig. 3. The device was fabricated on a silicon wafer and comprises of a 15 nm thin gold stripe long range plasmonic waveguide placed inside a thick Benzocy-Clobutene (BCB) layer. The principle of operation is based on voltage induced resistive heating of the gold stripe which in turn changes the optical transmission of the plasmonic mode via the thermo-optic effect. Based on this effect, the authors experimentally demonstrate an extinction ratio of 30 dB in a 5 mm long device. The modulation speed was around 1 ms with an energy consumption of 10 mW.

The performances of such devices was further improved by Gosciniak *et al*. [39]. In their device, they use a cycloaliphatic acrylate polymer layer as the active medium which has a higher thermo-optic coefficient compared to BCB. The authors experimentally demonstrate that the required length for complete modulation is around $L_\pi = 32.3$ μm, however, the –3 dB frequency cutoff of 10 kHz and power consumption of 1.7 mW is still a limitation of this approach.

Recently, the thermo-plasmonic effect was used in a device that can switch 4×10 Gbit/s traffic [44]. There, the thermo-plasmonic elements were fabricated into a Mach-Zehnder interferometer with dielectrically loaded SPP waveguides and passive silicon waveguides. The authors show a device with an active length of 60 μm, switching powers of 13.1 mW along with 3.8 μs response times.

IV. Free Carrier Dispersion Effect

The free carrier dispersion (or plasma dispersion) effect has been suggested as a promising approach for achieving high

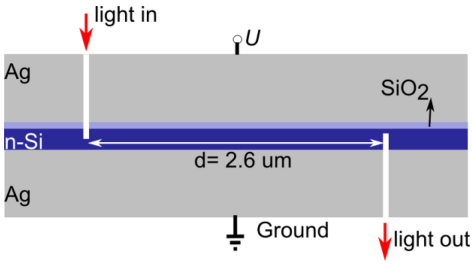

Fig. 4. Schematic cross section of interferometer based plasMOStor with silicon as an active medium [25].

speed plasmonic switching. In this effect, the induced free charges, n_c, cause changes of the imaginary and real part of the refractive index of the medium. These changes are predicted using the Drude model:

$$\varepsilon(\omega) = \varepsilon_\infty - \frac{\omega_p^2}{\omega(\omega + i\gamma)},\ \omega_p^2 = \frac{n_c e^2}{\varepsilon_0 m^*}$$

where γ is the electron scattering rate, ω is the angular frequency in rad/s, ε_0 is the free space permittivity, ε_∞ is the permittivity at infinity frequency, ω_p is the plasma frequency, m^* is the effective mass of electrons and e denotes the electron charge.

To this date, several demonstrations have been given in literature which are using the plasma dispersion effect for optical modulation. The "plasMOStor" [25], for the first time, demonstrated the potential of integrated plasmonics in an optical link. Fig. 4 shows a cross section of the fabricated device. It employs a four layer structure comprising of silver-oxide-silicon-silver that supports both photonic and plasmonic modes. The operation principle is based on a voltage induced free carrier injection which leads to refractive index change in silicon. This dispersion is used in an interferometeric structure formed by the two slots as shown in Fig. 4. When a voltage is applied the photonic and plasmonic mode in the cavity are perturbed resulting in a modulation of the transmitted optical signal of 3 to 4 dB in a device of 2.2 μm length. The operating voltage of the plasMOStor was measured to be 1 V. The device was tested to work at dc. However, the authors estimated the device to work in the GHz regime as the bandwidth will only be limited by the formation speed of the accumulation layer. A technological challenge of this approach is the potential high leakage current passing through the insulator due to indiffusion of Ag into the oxide layer. Leakage currents may lead to an early electrostatic break down behavior and may affect the reliability of the device.

In a recent article, Melikyan *et al.* [45] proposed a surface plasmon polariton absorption modulator (SPPAM) operating at 1.55 μm, Fig. 5. The operation principle of this device is based on the concept of epsilon near zero in ITO. Basically, the voltage-induced free carriers in ITO alter the real part of its permittivity between negative and positive values, which leads to strong changes in the absorption. A small signal modulation was demonstrated at a few 100 kHz—mostly limited by the RC constant of the electrical circuit.

More recently, Sorger *et al.* [46] built an SPPAM based on a similar structure. They experimentally showed successful switching operation with a 20 dB extinction ratio with 2 V_{pp} voltage in a device of 20 μm length. The frequency of operation of this device was several kHz. A difficulty of the SPPAM arises when the insulating oxide layer between the conductive contacts is getting very thin. Switching might then rely to a larger extent on the much slower electrochemical effect than the ultra-fast plasma dispersion effect, as will be outlined below.

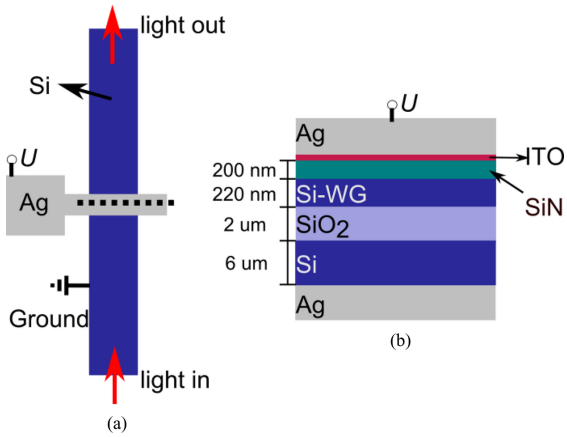

Fig. 5. Structure of the SPP absorption modulator based on ITO active layer [45].

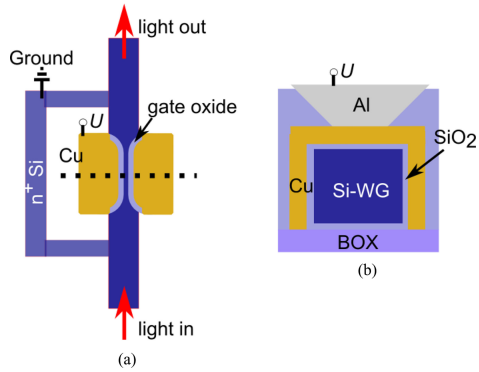

Fig. 6. Electro-absorption plasmonic modulator based on silicon active layer [47].

A similar approach using the free carrier absorption modulation effect in silicon rather than ITO was experimentally demonstrated in Ref. [47]. In this paper, the authors showed a Si nanoplasmonic electro-absorption modulator using copper as a metal electrode. The device is sketched in Fig. 6. According to the authors, the operation principle relies on the voltage induced carrier injection, which leads to an absorption change in silicon. However, the device dissipates a significant amount of power (0.1 mA in 2 μm^2) and therefore part of the modulation could also be due to thermal effects. The authors demonstrated a dc modulation with 3 dB extinction in a device of 4 μm length. The advantage of this structure is its compatibility with CMOS process technology. This comes at the price of a lower operation frequency as the transport velocity of the carriers in silicon are limited.

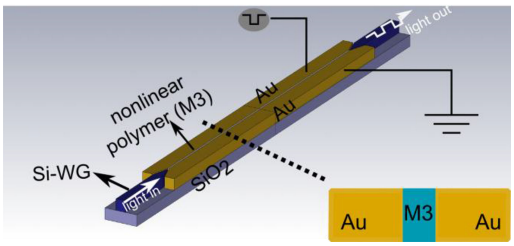

Fig. 7. Schematic of the PPM based on nonlinear materials [26].

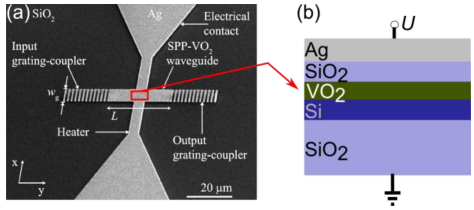

Fig. 8. (a) Top view SEM image of the plasmonic switch based on the phase change effect; (b) cross section of the active device [60].

V. Pockels Effect

The Pockels effect is another physical phenomenon employed in plasmonic switches. It is particularly well suited for achieving high data rate operation due to its instantaneous electro-optical coefficient. For practical reasons, plasmonic Pockels effect switches are usually based on the MIM structure. This way voltage can be simply applied across the metals. The refractive index changes Δn, via the Pockels effect are given by [48]:

$$\Delta n = \frac{1}{2} \times r_{33} n^3 \frac{U}{w}$$

where U/w (modulating voltage U, gap width w) is the static electric field and r_{33} is the electro-optical coefficient. The induced phase shift on the plasmonic mode can then be exploited for modulation in two different geometrical configurations: (a) the ring resonators; (b) the Mach-Zender interferometer.

In 2012, Randahawa *et al*. [49] experimentally demonstrated a plasmonic switch operated using the Pockels effect. The device consists of a dielectrically loaded plasmonic ring resonator. In this first demonstration, the extinction ratio (10%) and the switching speed (few seconds) were rather low. The latter was attributed to a dominating voltage induced electrostrictive effect of the host matrix.

Very recently, a 40 Gbit/s high-speed plasmonic modulator was experimentally demonstrated [26]. The device is based on the Pockels effect which comes from a nonlinear polymer infiltrated into the slot of the MIM waveguide. The device has a very flat frequency response up to 65 GHz, is 29 μm in length and features a power consumption of around 70 fJ/bit if operated with a U_{pp} of 4.7 V. The device operated reliably across a 120 nm wavelength window. It is noteworthy that the first plasmonic phase modulator (PPM) features a RF bandwidth that exceeds the bandwidth of known silicon modulators [50], [51], while its footprint remains among the smallest [11], [48], [52]. The plasmonic-photonic hybrid structure from Ref. [26] is schematically depicted in Fig. 7. The PPM was fabricated on an silicon-on-insulator (SOI) platform and consists of two horizontal metal taper slaps integrated with an SOI waveguide and a phase modulator. The light is guided through the SOI waveguide and then converted into a SPP. The SPP is then guided into the phase modulator section, which consists of two metal pads separated by a nanometer-scale vertical slot, see Fig. 7. The slot is filled with a nonlinear organic material, the refractive index n of which can be changed via the Pockels effect. By modulating the refractive index of the polymer in the slot, the information is encoded in the phase of the SPP. At the end of the modulator section, the SPP is back-converted into a photonic mode.

More recently, a fully integrated plasmonic Mach-Zehnder modulator has also been realized experimentally. The device operated at 72 Gbit/s, featured a length of 10 μm only and consumed as little as 20 fJ/bit [53].

VI. Phase Change Effect

The phase change effect refers to a transition from an amorphous to a crystalline structure of a material due to Joule heating [54]–[56]. This unique property has interesting applications. In particular, the phase change materials can be switched from a transparent insulator (amorphous phase) to an associated metal state. Such a phase change results in an enormous change of the imaginary and real part of the refractive index of the material. This effect can be used for optical switching. Transformation to the amorphous phase requires typically a few tens of nanoseconds, whereas the transformation back to the crystalline phase is on the order of few hundred nanoseconds. The devices, however, pose significant technological challenges among which are (a) high switching powers of a few mW and (b) resistance drifting. The latter is explained in literature by changes of the resistances with time which of course affect the reliability of the devices [57]–[59].

The plasmonic switches based on the phase change effect could be very interesting to reduce the characteristic length scale of MIM active plasmonic structure. For this, the phase change material has to be placed as an insulator between the two plasmonic metals, i.e., the place where the plasmonic field is largest. Thus, again there is an excellent overlap between the optical field and the index change material.

Vanadium dioxide has emerged as an attractive material with a phase change effect. The transition temperature between the crystalline and amorphous is occurring around 70 °C and the switching speed is in the order of nanoseconds when an electrical or thermal excitation source is used. An experimental demonstration of a VO_2 plasmonic switch is shown in Fig. 8, see Ref. [60]. The device consists of VO_2 placed between 820 nm SiO_2 and 300 nm of Ag. The Ag electrode was used both as a plasmonic waveguide metal and as a heating source. With this scheme the authors showed a rather high extinction ratio of 10.3 dB with a device of 5 μm length. The device however requires relatively high electrical powers to induce the thermal phase change (28 mW) and operates at moderate speed (few μs).

TABLE I
CHARACTERISTICS OF PLASMONIC SWITCHES

Optical Modulation Mechanism	THERMO-PLASMONIC [44]	Free Carrier Dispersion [46]	Pockels [53]	Phase Change [60]	ECM [62]
Length	60 [μm]	20 [μm]	5 [μm]	5 [μm]	10 [μm]
Extinction ratio	14 [dB]	19.1 [dB]	5.5 [dB]	10.3 [dB]	12 [dB]
Energy Consumption	13.1 [mW]	–	20 [fJ/bit]	28 [mW]	0.2 [μW]
Demonstrated Bandwidth	3.8 [MHz]	–	$>$75 [GHz]	[kHz]	[MHz]
Estimated upper Bandwidth	100 MHz	THz	THz	100 MHz	100 MHz

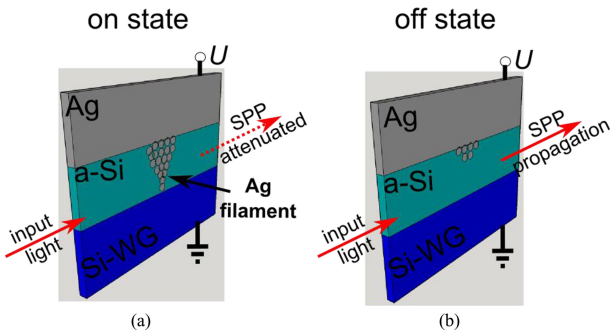

Fig. 9. (a) On state: formation of the metallic nanoscale filament; (b) off state: annihilation of the metallic nanoscale filament [61].

VII. ELECTROCHEMICAL METALIZAZATION (ECM) EFFECT

In ECM plasmonic devices or plasmonic memristors (resistor with memory characteristics), a voltage induced reversible filament formation inside the insulating layer of a plasmonic MIM waveguide is utilized to create two different distinct levels of optical transmission [61], [62]. This effect is rather unique for applications targeting ultra-small optical switches. The effect is large because of a perfect overlap between the induced nanofilament and the MIM plasmonic mode. Moreover this approach is ideal for ultralow power optical circuit switching because it can provide latching functionality, meaning that it can maintain the state without any energy. A challenge in fabrication is the control of the resistance instability, being at the origin of the uncontrollable morphology of the voltage induced nanofilament [63], [64]. So far, the memristive effect is heavily investigated for electronic memories [65]–[70] but it has only recently been discovered for plasmonic switching.

A first demonstration of the operation principle was given in Ref. [61]. The device consists of a vertical Ag/a-Si/p-Si structure butt-coupled to a single-mode SOI waveguide. The optical transmission via the plasmonic memristive device can be varied by switching the electrical resistance of a-Si where the switching mechanism is attributed to the formation/annihilation of nanoscale silver filaments [71]–[73], see Fig. 9. More precisely, under the application of a positive (negative) voltage at the silver electrode, silver ions infiltrated (retracted) the a-Si layer and formed (annihilated) a nanoscale conductive channel. Thus, the conduction mechanism is dominated by an enhanced (reduced) electron tunneling through this metal filament, i.e., the device is turned on (off) and the measured optical transmission is low (high) due to the increased (reduced) losses through absorption and scattering mechanisms. The authors managed to build a reversible nanofilament based plasmonic switch as a result of the variation of the absorption and scattering loss of the fundamental gap mode.

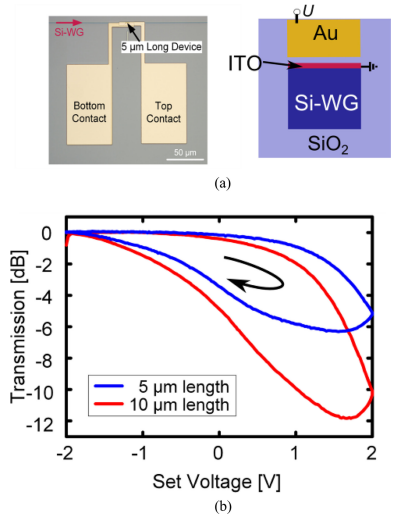

Fig. 10. (a) Left: optical microscope image top view of a fabricated 5 μm long device with silicon waveguide (Si-WG) and electrical contact pads; right: schematic cross section of the active plasmonic switch. (b) Optical transmission as a function of voltage showing a clear hysteresis and a latching switching ratio with an extinction ration of 12 dB in 10 μm long device.

Furthermore, the authors showed a reproducible and well defined nanoscale resistance switching characteristic with switching current of $\sim$35 nA at 4 V, power consumption on the order of 0.15 μW and an extinction ratio of few percent.

Only few months later, a significant advancement was reported demonstrating that the memristance effect might be of practical relevance [62]. In particular the authors showed an extinction ratio of 12 dB in a 10 μm long device. Again, the device exploits the reversible formation of conducting nanofilaments in a gold/silica/indium-tin-oxide plasmonic waveguide, Fig. 10(a). The device is integrated onto a silicon waveguide on a standard SOI wafer.

Fig. 10(b) shows how the optical switch changes from the "on" state to the "off" state when the voltage is increased from -2 V to $+2$ V. If the voltage is turned off (0 V), one can see how the device maintains its state. Only when the voltage is switched back to -2 V it returns back to the "on" state and again maintains this state even after the voltage is turned off again. As shown in 10(b), a repeatable and well defined hysteresis with a 12 dB extinction ratio is observed. This hysteresis is crucial for the latching functionality of the switch. The switching speed was also investigated. A sinusoidal modulation in the MHz regime

was applied to the device and detected with a photodiode and lock-in amplifier. This revealed a flat frequency response between 40 kHz and 10 MHz. Since electronic memristors show switching times below 10 ns [63], the authors expect that higher speeds should also be doable for plasmonic memristors by optimizing dimensions and material compositions.

VIII. Conclusions and Outlook

Electrically driven plasmonic modulators have seen significant progress over the past few years, see Table 1. Especially the prospect of a very small footprint and a low RC time constant has been and still is a driving factor for this field. Until recently, the modulation speed was often considered to be a limiting factor. However, with the recent experimental demonstration of modulation frequencies above 70 GHz, a power consumption of 20 fJ/bit, plasmonic modulators have now reached a very competitive performance level. In addition, concepts of a novel latching switch exploiting the phase change effect and ECM effect offer new venues for novel device and memory concepts.

The main issue with any kind of plasmonic device typically is the loss. This issue can only be addressed by either of two ways. The community finds a path towards a lower loss plasmonic device concept and some suggestions have already been made or the plasmonic losses are offset by the short length of highly nonlinear plasmonic devices.

In conclusion, the field of plasmonic modulators and switches has progressed dramatically over the past few years and we are looking forward to see more new and unique results.

References

[1] M. C. Wu, O. Solgaard, and J. E. Ford, "Optical MEMS for lightwave communication," *J. Lightw. Technol.*, vol. 24, no. 12, pp. 4433–4454, Dec. 2006.

[2] E. L. Wooten *et al.*, "A review of lithium niobate modulators for fiber-optic communications systems," *IEEE J. Sel. Topics Quantum Electron.*, vol. 6, no. 1, pp. 69–82, Jan./Feb. 2000.

[3] T. Fujiwara, A. Watanabe, and H. Mori, "Measurement of uniformity of driving voltage in Ti:$LiNbO_3$ waveguides using Mach-Zehnder interferometers," *IEEE Photon. Technol. Lett.*, vol. 2, no. 4, pp. 260–261, Apr.. 1990.

[4] M. M. Howerton, R. P. Moeller, A. S. Greenblatt, and R. Krahenbuhl, "Fully packaged, broad-band $LiNbO_3$ modulator with low drive voltage," *IEEE Photon. Technol. Lett.*, vol. 12, no. 7, pp. 792–794, Jul. 2000.

[5] G. T. Reed, G. Mashanovich, F. Y. Gardes, and D. J. Thomson, "Silicon optical modulators," *Nature Photon*, vol. 4, pp. 518–526, Jul. 2010.

[6] J. Leuthold *et al.*, "Silicon-organic hybrid electro-optical devices," *IEEE J. Sel. Topics Quantum Electron.*, vol. 19, no. 6, pp. 114–126, Nov./Dec. 2013.

[7] J. M. Brosi *et al.*, "High-speed low-voltage electro-optic modulator with a polymer-infiltrated silicon photonic crystal waveguide," *Opt Exp.*, vol. 16, pp. 4177–91, Mar. 2008.

[8] T. F. Krauss and R. M. De La Rue, "Photonic crystals in the optical regime—Past, present and future," *Prog. Quant. Electron.*, vol. 23, pp. 51–96, Mar. 1999.

[9] Q. Xu, B. Schmidt, S. Pradhan, and M. Lipson, "Micrometre-scale silicon electro-optic modulator," *Nature*, vol. 435, pp. 325–327, May 2005.

[10] B. Schmidt *et al.*, "Compact electro-optic modulator on silicon-on-insulator substrates using cavities with ultra-small modal volumes," *Opt. Exp.*, vol. 15, pp. 3140–8, Mar. 2007.

[11] E. Timurdogan *et al.*, "An ultralow power athermal silicon modulator," *Nature Commun.*, vol. 5, pp. 1–11, Jun. 2014.

[12] E. Ozbay, "Plasmonics: Merging photonics and electronics at nanoscale dimensions," *Science*, vol. 311, pp. 189–193, Jan. 2006.

[13] J. Leuthold *et al.*, "Plasmonic communications: Light on a wire," *Opt. Photon. News*, vol. 24, pp. 28–35, May 2013.

[14] W. L. Barnes, A. Dereux, and T. W. Ebbesen, "Surface plasmon subwavelength optics," *Nature*, vol. 424, pp. 824–830, Aug. 2003.

[15] T. Nikolajsen, K. Leosson, and S. I. Bozhevolnyi, "Surface plasmon polariton based modulators and switches operating at telecom wavelengths," *Appl. Phys. Lett.*, vol. 85, pp. 5833–5835, Dec. 2004.

[16] A. V. Krasavin, A. V. Zayats, and N. I. Zheludev, "Active control of surface plasmon–polariton waves," *J. Opt. A-Pure Appl. Op.*, vol. 7, p. S85, Oct. 2005.

[17] W. Cai, J. S. White, and M. L. Brongersma, "Compact, high-speed and power-efficient electrooptic plasmonic modulators," *Nano Lett.*, vol. 9, pp. 4403–4411, Dec. 2009.

[18] K. F. MacDonald, Z. L. Samson, M. I. Stockman, and N. I. Zheludev, "Ultrafast active plasmonics," *Nature Photon.*, vol. 3, pp. 55–58, Dec. 2009.

[19] I. Goykhman *et al.*, "Locally oxidized silicon surface-plasmon Schottky detector for telecom regime," *Nano Lett.*, vol. 11, pp. 2219–2224, Jun. 2011.

[20] P. Berini and I. De Leon, "Surface plasmon-polariton amplifiers and lasers," *Nature Photon.*, vol. 6, pp. 16–24, Dec. 2012.

[21] V. E. Babicheva *et al.*, "Towards CMOS-compatible nanophotonics: Ultra-compact modulators using alternative plasmonic materials," *Opt. Exp.*, vol. 21, pp. 27326–27337, Nov. 2013.

[22] J. A. Dionne, L. A. Sweatlock, H. A. Atwater, and A. Polman, "Plasmon slot waveguides: Towards chip-scale propagation with subwavelength-scale localization," *Phys. Rev. B*, vol. 73, p. 035407, Jan. 2006.

[23] M. W. Knight, H. Sobhani, P. Nordlander, and N. J. Halas, "Photodetection with active optical antennas," *Science*, vol. 332, pp. 702–704, May 2011.

[24] L. Novotny and N. Van Hulst, "Antennas for light," *Nature Photon.*, vol. 5, pp. 83–90, Feb. 2011.

[25] J. A. Dionne, K. Diest, L. A. Sweatlock, and H. A. Atwater, "PlasMOStor: A metal−oxide−Si field effect plasmonic modulator," *Nano Lett.*, vol. 9, pp. 897–902, Feb. 2009.

[26] A. Melikyan *et al.*, "High-speed plasmonic phase modulators," *Nature Photon.*, vol. 8, pp. 229–233, Feb. 2014.

[27] K. C. Y. Huang *et al.*, "Electrically driven subwavelength optical nanocircuits," *Nature Photon.*, vol. 8, pp. 244–249, Mar. 2014.

[28] P. Berini, "Long-range surface plasmon polaritons," *Adv. Opt. Photon.*, vol. 1, pp. 484–588, Nov. 2009.

[29] T. Holmgaard, S. I. Bozhevolnyi, L. Markey, and A. Dereux, "Dielectric-loaded surface plasmon-polariton waveguides at telecommunication wavelengths: Excitation and characterization," *Appl. Phys. Lett.*, vol. 92, p. 011124, Nov. 2008.

[30] R. M. Briggs *et al.*, "Efficient coupling between dielectric-loaded plasmonic and silicon photonic waveguides," *Nano Lett.*, vol. 10, pp. 4851–4857, Dec. 2010.

[31] C. Delacour *et al.*, "Efficient directional coupling between silicon and copper plasmonic nanoslot waveguides: Toward metal−oxide−silicon nanophotonics," *Nano Lett.*, vol. 10, pp. 2922–2926, Aug. 2010.

[32] A. Kumar *et al.*, "Dielectric-loaded plasmonic waveguide components: Going practical," *Laser Photon. Rev.*, vol. 7, pp. 938–951, Feb. 2013.

[33] A. Emboras *et al.*, "Efficient coupler between silicon photonic and metal-insulator-silicon-metal plasmonic waveguides," *Appl. Phys. Lett.*, vol. 101, p. 251117, Dec. 2012.

[34] A. Emboras *et al.*, "MNOS stack for reliable, low optical loss, Cu based CMOS plasmonic devices," *Opt. Exp.*, vol. 20, pp. 13612–21, Jun. 2012.

[35] T. Holmgaard and S. I. Bozhevolnyi, "Theoretical analysis of dielectric-loaded surface plasmon-polariton waveguides," *Phys. Rev. B*, vol. 75, p. 245405, Jun. 2007.

[36] A. Melikyan *et al.*, "Photonic-to-plasmonic mode converter," *Opt. Lett.*, vol. 39, pp. 3488–3491, Jun. 2014.

[37] G. Gagnon, N. Lahoud, G. A. Mattiussi, and P. Berini, "Thermally activated variable attenuation of long-range surface plasmon-polariton waves," *J. Lightw. Technol.*, vol. 24, no. 11, pp. 4391–4402, Nov. 2006.

[38] J. Gosciniak *et al.*, "Thermo-optic control of dielectric-loaded plasmonic waveguide components," *Opt. Exp.*, vol. 18, pp. 1207–1216, Jan. 2010.

[39] J. Gosciniak, L. Markey, A. Dereux, and S. I. Bozhevolnyi, "Efficient thermo-optically controlled Mach-Zhender interferometers using dielectric-loaded plasmonic waveguides," *Opt. Exp.*, vol. 20, pp. 16300–16309, Jul. 2012.

[40] J. Gosciniak and S. I. Bozhevolnyi, "Performance of thermo-optic components based on dielectric-loaded surface plasmon polariton waveguides," *Sci. Rep.*, vol. 3, pp. 1–8, Aug. 2013.

[41] J. C. Weeber *et al.*, "Nanosecond thermo-optical dynamics of polymer loaded plasmonic waveguides," *Opt. Exp.*, vol. 21, pp. 27291–27305, Nov. 4, 2013.
[42] M. G. Nielsen *et al.*, "Silicon-loaded surface plasmon polariton waveguides for nanosecond thermo-optical switching," *Opt. Lett.*, vol. 39, pp. 2282–2285, Apr. 2014.
[43] H. Fan, R. Charbonneau, and P. Berini, "Long-range surface plasmon triple-output Mach-Zehnder interferometers," *Opt. Exp.*, vol. 22, pp. 4006–4020, Feb. 2014.
[44] S. Papaioannou *et al.*, "Active plasmonics in WDM traffic switching applications," *Sci. Rep.*, vol. 2, pp. 652–666, Sep. 12, 2012.
[45] A. Melikyan *et al.*, "Surface plasmon polariton absorption modulator," *Opt. Exp.*, vol. 19, pp. 8855–8869, Apr. 2011.
[46] V. J. Sorger, D. Lanzillotti-Kimura Norberto, R.-M. Ma, and X. Zhang, "Ultra-compact silicon nanophotonic modulator with broadband response," *J. Nanophotonics*, vol. 1, pp. 17–22, Jul. 2012.
[47] S. Zhu, G. Q. Lo, and D. L. Kwong, "Electro-absorption modulation in horizontal metal-insulator-silicon-insulator-metal nanoplasmonic slot waveguides," *Appl. Phys. Lett.*, vol. 99, p. 151114, Sep. 2011.
[48] J.-M. Brosi *et al.*, "High-speed low-voltage electro-optic modulator with a polymer-infiltrated silicon photonic crystal waveguide," *Opt. Exp.*, vol. 16, pp. 4177–4191, Mar. 2008.
[49] S. Randhawa *et al.*, "Performance of electro-optical plasmonic ring resonators at telecom wavelengths," *Opt. Exp.*, vol. 20, pp. 2354–2362, Jan. 2012.
[50] L. Liao *et al.*, "40 Gbit/s silicon optical modulator for highspeed applications," *Electron. Lett.*, vol. 43, no. 22, pp. 1196–1197, Oct. 2007.
[51] D. J. Thomson *et al.*, "50-Gb/s silicon optical modulator," *IEEE Photon. Technol. Lett.*, vol. 24, no. 4, pp. 234–236, Jan. 2012.
[52] H. C. Nguyen, S. Hashimoto, M. Shinkawa, and T. Baba, "Compact and fast photonic crystal silicon optical modulators," *Opt. Exp.*, vol. 20, pp. 22465–22474, Sep. 2012.
[53] C. Haffner *et al.*, "High-speed plasmonic Mach-Zehnder modulator in a waveguide," in *Proc. Eur. Conf. Opt. Commun.*, Cannes, France, 2014, pp. 1–3.
[54] R. M. Briggs, I. M. Pryce, and H. A. Atwater, "Compact silicon photonic waveguide modulator based on the vanadium dioxide metal-insulator phase transition," *Opt. Exp.*, vol. 18, pp. 11192–11201, May 2010.
[55] A. Kiouseloglou *et al.*, "A novel programming technique to boost low-resistance state performance in Ge-Rich GST phase change memory," *IEEE Trans. Electron Devices*, vol. 61, no. 5, pp. 1246–1254, May 2014.
[56] L. Perniola *et al.*, "Electrical behavior of phase-change memory cells based on GeTe," *IEEE Electron Device Lett.*, vol. 31, no. 5, pp. 488–490, May 2010.
[57] N. Papandreou *et al.*, "Drift-tolerant multilevel phase-change memory," in *Proc. 3rd IEEE Int. Memory Workshop* , 2011, pp. 1–4.
[58] N. Papandreou *et al.*, "Drift-resilient cell-state metric for multilevel phase-change memory," in *Proc. IEEE Int. Electron Dev. Meeting*, 2011, pp. 3.5.1–3.5.4.
[59] D. Krebs *et al.*, "Changes in electrical transport and density of states of phase change materials upon resistance drift," *New J. Phys.*, vol. 16, p. 043015, Apr. 2014.
[60] A. Joushaghani *et al.*, "Sub-volt broadband hybrid plasmonic-vanadium dioxide switches," *Appl. Phys. Lett.*, vol. 102, p. 061101, Feb. 2013.
[61] A. Emboras *et al.*, "Nanoscale plasmonic memristor with optical readout functionality," *Nano Lett.*, vol. 13, pp. 6151–6155, Dec. 2013.
[62] C. Hoessbacher *et al.*, "The plasmonic memristor: A latching optical switch," *Optica*, vol. 1, pp. 198–202, Oct. 2014.
[63] R. Waser, R. Dittmann, G. Staikov, and K. Szot, "Redox-based resistive switching memories—Nanoionic mechanisms, prospects, and challenges," *Adv. Mater.*, vol. 21, pp. 2632–2663, Jul. 2009.
[64] Y. Yang *et al.*, "Electrochemical dynamics of nanoscale metallic inclusions in dielectrics," *Nature Commun.*, vol. 5, pp. 4232–4241, Jun. 2014.
[65] D. B. Strukov, G. S. Snider, D. R. Stewart, and R. S. Williams, "The missing memristor found," *Nature*, vol. 453, pp. 80–83, May 2008.
[66] K. Terabe, T. Hasegawa, T. Nakayama, and M. Aono, "Quantized conductance atomic switch," *Nature*, vol. 433, pp. 47–50, Jan. 2005.
[67] R. Waser and M. Aono, "Nanoionics-based resistive switching memories," *Nature Mater.*, vol. 6, pp. 833–840, Nov. 2007.
[68] J.-Y. Chen *et al.*, "Dynamic evolution of conducting nanofilament in resistive switching memories," *Nano Lett.*, vol. 13, pp. 3671–3677, Aug. 2013.
[69] J. J. Yang *et al.*, "Memristive switching mechanism for metal-oxide-metal nanodevices," *Nature Nano*, vol. 3, pp. 429–433, Jul. 2008.
[70] J. J. Yang *et al.*, "The mechanism of electroforming of metal oxide memristive switches," *Nanotechnology*, vol. 20, p. 215201, 2009.
[71] A. E. Owen, J. Hu, J. Hajto, and A. J. Snell, "Electronic switching in amorphous silicon devices: Properties of the conducting filament," in *Proc. 5th Int. Conf. Solid-State Integr. Circuit Technol.* , 1998, pp. 830–833.
[72] A. Avila and R. Asomoza, "Switching in coplanar amorphous hydrogenated silicon devices," *Solid-State Electron.*, vol. 44, pp. 17–27, Jan. 2000.
[73] Y. Yang *et al.*, "Observation of conducting filament growth in nanoscale resistive memories," *Nature Commun.*, vol. 3, p. 732, Mar. 2012.

Alexandros Emboras received the degree from the Physics Department, University of Patras, Patras, Greece, and the Ph.D. degree from CEA-LETI, Grenoble, Germany. His thesis was focused on the design and fabrication of CMOS plasmonic modulators. He joined in November 2013 as a Senior Researcher at the Institute of Electromagnetic Fields Group, ETH Zürich, Zürich, Switzerland. Prior to that, he was a Postdoctoral Researcher in the optoelectronics group at Hebrew University of Jerusalem. His current research interests include the design and fabrication of novel atomic scale plasmonic devices.

Claudia Hoessbacher was born in Erlenbach a. M., Germany, in 1987. She received the B.Sc. degree in electrical engineering and the M.Sc. degree in optics and photonics from Karlsruhe Institute of Technology, Karlsruhe, Germany, in 2010 and 2012, respectively. She is currently working toward the Ph.D. degree in the field of plasmonic switches and modulators in the Institute of Electromagnetic Fields, ETH Zürich, Zürich, Switzerland.

Christian Haffner received the Master degree in electrical engineering from the Karlsruhe Institute of Technology, Karlsruhe, Germany, and is currently working toward the Ph.D. degree at the Swiss Federal Institute of Technology, Zürich, Switzerland. His research interests include nonlinear optical effects in plasmonic structures.

Wolfgang Heni received the M.Sc. degree in electrical engineering from the Karlsruhe Institute of Technology, Karlsruhe, Germany, in 2013. During his thesis, he worked in organic electro-optic switches and modulators in silicon. He is currently working toward the Ph.D. degree in electrical engineering at ETH Zürich, Zürich, Switzerland. He is a Research Associate at the Institute of Electromagnetic Fields, ETH Zürich. His research interests include integrated plasmonic and photonic devices.

Ueli Koch received the M.Sc. degree in computational science and engineering from ETH Zürich, Zürich, Switzerland, in 2013. He is currently working toward the Ph.D. degree in the Institute of Electromagnetic Fields at ETH Zürich. His current research interests include the numerical modeling and simulation of surface effects in plasmonic nanostructures with a particular focus on electro-optic modulation.

Ping Ma received the B.E. degree from Tianjin University, Tianjin, China in 2003, the M.Sc. degree from the Royal Institute of Technology, Stockholm, Sweden in 2005, and the D.Sc. degree from the Swiss Federal Institute of Technology Zürich (ETH), Zürich, Switzerland in 2011, all in electronic engineering. His doctoral thesis studied photonic bandgap structures with TM-bandgap for ultrafast all-optical switches based on intersubband transition in InGaAs/AlAsSb quantum wells. After a short postdoctoral research stay at ETH Zürich, he worked at Oracle Labs in San Diego, CA, USA, where he performed research on ferroelectric materials for spectral tuning of ring resonators and novel electro-optic modulators for silicon photonic interconnects, He has recently returned to ETH Zürich and joined in Prof. Jürg Leuthold's institute as a Senior Research Scientist. He is the author or coauthor of 14 publications and holds one pending patent.

Yuriy Fedoryshyn received the Master degree in laser and optoelectronic technology from Lviv Polytechnic National University, Lviv, Ukraine, in December 2002, and the Ph.D. degree from ETH Zürich, Zürich, Switzerland, in February 2012. His Master thesis, conducted in the Group of Mesoscopic Physics, University of Neuchatel, Neuchatel, Switzerland, was focused on development of Ge-based waveguides for quantum cascade lasers. His PhD thesis, performed in the Communication Photonics Group at the Electronics Laboratory of ETH Zürich, was concentrated on modeling, growth, and characterization of InGaAs/AlAsSb quantum well structures for ultrafast all-optical switching based on intersubband transitions. In October 2012, he joined the Institute of Electromagnetic Fields at ETH Zürich, where his current research activities are focused on integrated photonic, plasmonic, and optoelectronic devices.

Jens Niegemann received the Dipl. Phys. degree in 2004 from the Universität Karlsruhe, Karlsruhe, Germany. In 2009, he received the Ph.D. degree from the Karlsruhe Institute of Technology (KIT). From 2009 to 2011, he lead the Young Investigator Group "Computational Nano-Photonics" at the KIT. He joined the Institute of Electromagnetic Fields at ETH Zürich, Zürich, Switzerland as a Postdoctoral Researcher in 2011. His research interests include the theoretical and numerical analysis of electromagnetic wave propagation in nanostructured media.

Christian Hafner received the Ph.D. degree from ETH Zürich, Zürich, Switzerland, for a proposition of a new method for computational electromagnetics, the multiple multipole program (MMP) in 1980. This method was also the main part of his habilitation on computational electromagnetics at ETH in 1987. It was honored by a Seymour Cray award for scientific computing in 1990. In 1999, he was given the title of Professor at ETH; and in 2010–2013, he was the Head at the Electromagnetic Fields and Microwave Electronics Laboratory at ETH. The focus of his current research is on the improvement, optimization, and generalization of numerical techniques of computational electromagnetics; the design and application of intelligent optimization procedures based on nature-inspired strategies; design and applications of metamaterials ranging from very low up to optical frequencies, plasmonics and optical antennas, scanning nearfield microscopy, solar cells, etc. His work was published in various international journals papers, as well as in seven books and book-software packages, which include his 2-D-MMP, 3-D-MMP, and MaX-1 codes. The latest MMP codes and 2-D and 3-D finite-difference time domain codes and are also available in the open source package OpenMaXwell.

Juerg Leuthold (F'13) received the Ph.D. degree in physics from the Swiss Federal Institute of Technology (ETH), Zürich, Switzerland, in 1998. From 1999 to 2004, he was with Bell Labs, Lucent Technologies in Holmdel, NJ, USA, where he has been performing device and system research. From July 2004 to February 2013, he was a Full Professor at the Karlsruhe Institute of Technology, where he was the Head of the Institute of Photonics and Quantum Electronics, and the Head of the Helmoholtz Research Institute of Micro Structure Technology. Since March 2013, he has been a Full Professor at ETH Zürich. Dr. Leuthold is a Fellow of the Optical Society of America and also a member of the Heidelberg Academy of Science.